# A new predictive dynamic model describing the effect of the ambient temperature and the convective heat transfer coefficient on bacterial growth

Hana Ben Yaghlene, Ivan Leguérinel, Moktar Hamdi, Pierre Mafart

# A new predictive dynamic model describing the effect of the ambient temperature and the convective heat transfer coefficient on bacterial growth

H. Ben Yaghlene[a,b*], I. Leguerinel[a], M. Hamdi[b], P. Mafart[a]

[a]: Université Européenne de Bretagne, EA3882, Laboratoire Universitaire de Biodiversité et Ecologie Microbienne, IFR148 ScInBioS, Université de Bretagne Occidentale, 6 rue de l'université, F29334 Quimper, Cedex, France

[b]: Laboratoire d'Ecologie et de Technologie Microbienne, Institut National des Sciences Appliquées et de Technologie (INSAT), 2 Boulevard de la terre, B.P. 676, 1080 Tunis, Tunisie

[*]Corresponding author: LUBEM, UBO, 6 rue de l'Université, F29334, Quimper Cedex, France. Tel.: +33 2 98 90 02 27; Fax: +33 2 98 90 85 44

E mail address: hana.benyaghlene@univ-brest.fr

**Abstract**

In this study, predictive microbiology and food engineering were combined in order to develop a new analytical model predicting the bacterial growth under dynamic temperature conditions. The proposed model associates a simplified primary bacterial growth model without lag, the secondary Ratkowsky "square root" model and a simplified two-parameter heat transfer model regarding an infinite slab. The model takes into consideration the product thickness, its thermal properties, the ambient air temperature, the convective heat transfer coefficient and the growth parameters of the micro organism of concern. For the validation of the overall model, five different combinations of ambient air temperature (ranging from 8 °C to 12 °C), product thickness (ranging from 1 cm to 6 cm) and convective heat transfer coefficient (ranging from 8 W/($m^2$.K) to 60 W/($m^2$.K)) were tested during a cooling

procedure. Moreover, three different ambient air temperature scenarios assuming alternated cooling and heating stages, drawn from real refrigerated food processes, were tested. General agreement between predicted and observed bacterial growth was obtained and less than 5% of the experimental data fell outside the 95 percent confidence bands estimated by the bootstrap percentile method, at all the tested conditions. Accordingly, the overall model was successfully validated for isothermal and dynamic refrigeration cycles allowing for temperature dynamic changes at the centre and at the surface of the product. The major impact of the convective heat transfer coefficient and the product thickness on bacterial growth during the product cooling was demonstrated. For instance, the time needed for the same level of bacterial growth to be reached at the product's half thickness was estimated to be 5 and 16.5 h at low and high convection level, respectively. Moreover, simulation results demonstrated that the predicted bacterial growth at the air ambient temperature cannot be assumed to be equivalent to the bacterial growth occurring at the product's surface or centre when convection heat transfer is taken into account. Our results indicate that combining food engineering and predictive microbiology models is an interesting approach providing very useful tools for food safety and process optimisation.

**Key words:**

Predictive microbiology; Heat transfer; Dynamic models; Bacterial growth; Cooling; Heating.

## Nomenclature

| | |
|---|---|
| $A$ | Transfer area ($m^2$) |
| $Bi$ | Biot number |
| $E$ | Product thickness (m) |
| $f'$ | Thermal proliferation value |
| $Fo$ | Fourier number |
| $h$ | Convective heat transfer coefficient ($W/(m^2.K)$) |
| $j$ | Lag factor for reduced temperature profile |
| $k$ | Slope of the linear portion of the semi-logarithmic plot of reduced temperature *vs* time. |
| $l$ | Characteristic dimension (m) |
| $N$ | Microbial cell density at time t (CFU/mL) |
| $N_0$ | Initial microbial cell density (CFU/mL) |
| $O$ | Observed microbial cell density ($\log_{10}$ CFU/mL) |
| $OD$ | Microbial optical density at time t |
| $OD_0$ | Initial microbial optical density |
| $P$ | Predicted microbial cell density ($\log_{10}$ CFU/mL) |
| $t$ | Time (s) |
| $T$ | Temperature of the product (°C) |
| $T_{eq}$ | Equivalent temperature |
| $T_{min}$ | Temperature below which no microbial growth occurs (°C) |
| $T_{opt}$ | Temperature at which the microbial growth is optimal (°C) |
| $T_0$ | Initial product temperature (°C) |
| $T_\infty$ | Ambient temperature (°C) |
| $x$ | Distance from the centre (m) |
| $x_{max}$ | Half-thickness for an infinite slab (m) |
| $\alpha$ | Thermal diffusivity of the product ($m^2/s$) |
| $\Gamma$ | Overall gamma function |
| $\gamma$ | Thermal gamma function |
| $\lambda$ | Thermal conductivity of the product (W/(m.K)) |
| $\mu$ | Specific microbial growth rate ($h^{-1}$) |
| $\mu_{opt}$ | Optimal specific microbial growth rate ($h^{-1}$) |
| $\varphi$ | First root of cot $\varphi = \varphi / Bi$ |
| $\varphi_n$ | Roots of cot $\varphi = \varphi / Bi$ |

## 1. Introduction

Predictive food microbiology involves knowledge of microbial growth responses to environmental factors expressed in quantitative terms by mathematical equations (models) (McMeekin et al., 1997). It is generally agreed that the most important environmental factor that affects bacterial growth in food is temperature. This factor is constantly changing during processing, storage and distribution of food products (Fujikawa et al., 2004). At the same time, control organizations propose stringent requirements regarding monitoring of the internal temperature of products being processed. For instance, according to the United States Department of Agriculture, the allowable growth of *Clostridium perfringens* during the cooling of certain meat and poultry products should be limited to 1 log (U.S.D.A, 1999). In the case of cured products, the guidelines recommend that products' internal temperature should be reduced from 54.4 °C to 26.6 °C in less than 5 h, and from 26.6 °C to 7.2 °C in the next 10 h (15 h total cooling time).

Predictive microbiology is a useful tool for assessing and controlling food safety particularly when models are able to cope with dynamic conditions such as changing temperatures. Numerous published models, reported in Table 1, have dealt with the prediction of bacterial growth under dynamic temperature conditions. Generally, these works were based on predictive models corresponding to isothermal bacterial growths which were modified in order to consider the effect of temperature changes. These studies primarily aimed at assessing the feasibility of predicting the bacterial growth at changing temperature. Indeed, predicting bacterial growth under dynamic conditions has been shown to be possible via the dynamic transformation of existing static models. According to the authors of the cited studies (Table 1), the models' predictions agreed well with experimental results after temperature changes.

Nevertheless, the considered scenarios of changing temperatures within bacterial models were various. In some cases, typical temperature profiles were considered either by the use of hypothetical ones or by the adoption of real temperature scenarios recorded while the studied products had been processed. In other cases, temperature profiles were simulated from heat transfer models. Mathematical models that integrate effectively heat transfer phenomena and dynamic bacterial growth relationships are scarce (Amezquita et al., 2005; de Jong et al., 2005; Zwietering and Hasting, 1997). Armitage (1997) derived the temperature histories for the deep leg and leg surface of a lamb carcass by using finite element models for dealing with regular shapes. Temperature function integration technique (TFI) was applied to the calculated temperature histories of five different cooling processes to simulate *Escherichia coli* growth on the leg surface of each carcass during aging. TFI technique was previously introduced by Gill and Harrison (1985). Data related to the growth of six strains of *E. coli* isolated from commercially packed livers were fitted according to the Ratkowsky model (Ratkowsky et al., 1982) linking the growth rate to temperature. Total growth was obtained by summation of partial growth calculated within sequential 3.75-min periods from the growth rate for the average temperature within each period. Estimated bacterial growth during offals cooling (cooling profiles were directly recorded on several offals being chilled) agreed well with observed data with *E. coli*. Bellara et al. (2000) experimentally validated bacterial growth modelling involving a heat transfer model of temperature fluctuations within a solid object. From data related to *E. coli* W3110 growth in agar, a model was set up describing bacterial growth as a function of temperature. This was then used in conjunction with a finite difference heat transfer model describing temperature change in a cylinder in order to calculate the bacterial growth that occurs in agar gel inside a cylindrical glass vessel under conduction cooling. Excellent agreement was found between model simulations and experimental data. Alavi et al. (2001) determined the growth characteristics of *Listeria*

98 *monocytogenes* in sterilized whole milk. The parameter values of the Baranyi dynamic growth
99 model (Baranyi et al., 1995) were determined. Finite element software, ANSYS, was
100 implemented to determine temperature distributions in milk cartons subject to a time-varying
101 ambient temperature profile. The space-time-temperature data were input to the Baranyi
102 dynamic growth model, to predict the microbial population density distribution and the
103 average population density in the milk carton. Amezquita et al. (2005) developed a computer
104 simulation scheme to analyze heat transfer phenomena and temperature-dependent *C.*
105 *perfringens* growth during cooling of cooked boneless cured ham. The temperature history of
106 ham was predicted from a finite element heat diffusion model. For *C. perfringens* growth, a
107 dynamic model was developed from the Baranyi's nonautonomous differential equation
108 (Baranyi and Roberts, 1994). The bacterium's growth model was integrated into the computer
109 program taking predicted temperature histories as input values. Validation of the model
110 predictions considered three different time–temperature cooling histories from 54.4 °C to 7.2
111 °C of the geometrical centre of a large cooked boneless ham. In a further work (Corradini et
112 al., 2006), the same data were fitted with the ad hoc empirical models in order to define the
113 three parameters temperature dependence of the modified version of the logistic primary
114 model. The continuous rate equation was solved incrementally by a numerical procedure
115 implemented in general purpose software. In both Amezquita et al. (2005) and Corradini et al.
116 (2006) works, predicted *C. perfringens* growth curves obtained from dynamic modelling
117 showed good agreement with observed results for the tested cooling scenarios. The integrated
118 modelling approach for predicting microbial behaviour during processing was reviewed by
119 Lebert and Lebert (2006).
120 Combination of predictive microbiology and food engineering allows both the assessment of a
121 process in relation to risk and its optimisation (Mafart, 2005). In spite of all the advances
122 made in modelling microbial growth, proposing and improving new overall models which

combine predictive microbiology and heat transfer phenomena is an obvious necessity. The more simple the proposed models and the more realistic the considered conditions are, the easiest is their implementation to food processes.

In the present study, we aimed to develop a new analytical model combining bacterial growth prediction and food engineering. Our goal was for the overall model to be simple and robust, with minimum involved parameters, and to integrate the process conditions. The proposed model is the association of three equations: a simplified primary model consisting of a simple exponential growth equation without lag time, the Ratkowsky "square root" model linking the specific growth rate to temperature (Ratkowsky et al., 1982), and a simplified two-parameter heat transfer model regarding an infinite slab. While classical models assume that ambient temperature is immediately reached at the growth medium, this work takes into account, not only the air temperature, but also the thickness of the medium, its thermal properties and the convective heat transfer coefficient. In addition, the proposed model may be easily implemented to various micro organisms having known growth parameters.

## 2. Development of the model

### 2.1. Heat transfer modelling

All cooling processes for solid materials exhibit similar behaviour. After an initial 'lag', the reduced temperature at the thermal centre of the food item decreases exponentially. The linear portion of the cooling curve (obtained by plotting, on semi-logarithmic axes, the reduced temperature $(T_\infty - T)/(T_\infty - T_0)$ versus time (Becker and Fricke, 2004), see Fig. A1 in the appendix) can typically be described by the simplified linear asymptotic form of the general heat transfer model, valid for Fourier number $Fo \geq 0.2$ with $Fo = \alpha \cdot t / l^2$ where $\alpha$ is thermal diffusivity of the product, $l$ is the characteristic dimension of the product, $T$ is the local temperature of the product at the time $t$, $T_0$ is the initial temperature of the product, $T_\infty$ is the

147 cooling medium temperature (pulsed air). Consequently, the heating or cooling kinetic is
148 expressed as follows:

149 $$T = T_{\infty}\left(1 - je^{-kt}\right) + T_0\, je^{-kt} \qquad (1)$$

150 Where $j$ is the lag factor and $k$ is the slope of the linear portion of the semi-logarithmic plot of
151 reduced temperature *vs* time. The value of the parameter $k$ depends upon the product shape, $l$,
152 $\alpha$ and the Biot number $Bi = hl/\lambda$, where $h$ is the convective heat transfer coefficient between
153 the product surface area and the ambient air and $\lambda$ is the thermal conductivity of the product.
154 A low Biot number ($Bi$ < 0.1) indicates that the internal resistance to heat transfer is
155 negligible, and thus, the temperature within the object is uniform at any given instant in time
156 while the external thermal resistance can be neglected for $Bi$ > 40 (Mafart, 1997).
157 The governing differential equation for infinite slab is given as follows with the initial
158 (uniform distribution of temperature) and boundary condition (surface convection):

159 $$\frac{\partial T}{\partial t} = \alpha \frac{\partial^2 T}{\partial x^2} \qquad (2)$$

160 where $x$ is distance from the centre. For initial condition of uniform temperature and boundary
161 conditions of central symmetry and convective heat transfer at the surface, solution for Eq. (2)
162 is supplied by the infinite series given by Carslaw and Jaeger (1986) (see Eq. (20) in the
163 appendix). It is a general knowledge that use of the first term of this series would be enough
164 when the Fourier number is greater than 0.2 since the temperature change after that certain
165 time would be linear (Becker and Fricke, 2004; Bimbenet et al., 2002; Caro-Corrales et al.,
166 2002; Dincer, 1996; Erdogdu, 2005). As long as the thermal diffusivity is constant, this first
167 term approach may be easily used to determine the temperature change with Eq. (1) and with
168 the known heat transfer coefficient value:
169 $k = \varphi^2.\alpha/l^2$ at any given position in the infinite slab where $\varphi$ is the first root of the following
170 equation:

171 $$\cot\varphi = \frac{\varphi}{Bi} \quad (3)$$

172 At the half thickness of the infinite slab,

173 $$j = \frac{2\sin\varphi}{\varphi + \sin\varphi\cos\varphi} \quad (4a)$$

174 At the surface of the infinite slab,

175 $$j = \frac{2\sin\varphi\cos\varphi}{\varphi + \sin\varphi\cos\varphi} \quad (4b)$$

176 With respect to the cooling/heating of the product during the initial 'lag' period (*Fo* < 0.2), we
177 assumed a straight linear link between $T_0$ and temperature at time corresponding to *Fo* = 0.2.

178 **2.2. Bacterial growth modelling**

179 As a primary model, a simple exponential growth without lag time was assumed:

180 $$N = N_0 e^{\mu t} \quad (5)$$

181 Where *N* is the cell number at time *t*, $N_0$ is the initial cell number and $\mu$ the specific bacterial
182 growth rate at time *t*.

183 The gamma function corresponds to a comparison between the growth rate of microbial cells
184 growing at given environmental conditions and the optimum growth rate that would be
185 measured at optimal conditions (Zwietering et al., 1992):

186 $$\Gamma = \frac{\mu}{\mu_{opt}} \quad (6)$$

187 In the framework of standard calculations aiming to compare processes to each others, a
188 simplified gamma function depending only on temperature can be derived from the "square
189 root" model of Ratkowsky et al. (1982) modified by Zwietering et al. (1992)

190 $$\gamma(T) = \left(\frac{T - T_{\min}}{T_{opt} - T_{\min}}\right)^2 \quad (7)$$

Where $T_{min}$ is the temperature below which no microbial growth occurs and $T_{opt}$ is the temperature at which the microbial growth is optimal.

If a process has to be intrinsically assessed regardless of the characteristics of the foodstuff, a partial proliferation value may be involved. If the local temperature at which the bacteria are growing is the single considered factor, Mafart (2005) defined a "thermal proliferation value" as:

$$f' = \int_0^t \gamma(T)\, dt \qquad (8)$$

This value has the dimension of a time and corresponds to a time-temperature cycle that would yield the same proliferation ratio than a growth of *f'* units of time at the optimal and constant temperature (Mafart, 2005).

The original differential form of equation (6) is:

$$\frac{1}{N}\frac{d(N)}{dt} = \mu(t) = \mu_{opt}\gamma[T(t)] \qquad (9)$$

the solution of which yields:

$$\frac{N}{N_0} = \exp\left[\mu_{opt}\int_0^t\left(\frac{T - T_{\min}}{T_{opt} - T_{\min}}\right)^2 dt\right] \qquad (10)$$

This model can be easily combined with heat transfer models permitting the obtainment of an analytic solution yielding the overall model. Note that, even for complex foodstuff shapes, an analytic solution of the model is possible, provided that thermal parameters of equation (1) (*j* and *k*) can be empirically determined from a temperature registration and a linear regression of reduced temperature.

The concept of thermal proliferation value may be usefully completed by that of equivalent temperature, which corresponds to the constant temperature that would yield the same proliferation during the duration of a thermal cycle. A cooling/heating process can then be

213 characterised and be compared with others by its duration and its equivalent temperature
214 (Mafart, 2005).

215 $$\gamma(T_{eq})t = f' \qquad (11)$$

216 where time is expressed in hours. The combination of this last equation with Eq. (7) yields:

217 $$T_{eq} = T_{\min} + (T_{opt} - T_{\min})\sqrt{\frac{f'}{t}} \qquad (12)$$

218 **2.3. Overall model**

219 The overall model developed in the present study aims to consider the convective heat
220 transfer coefficient and the temperature of the ambient medium when predicting bacterial
221 growth under dynamic conditions of temperature.

222 Combining Eqs. (1) and (7) the obtained time-dependent $\gamma(T)$ function is employed in Eq. (8)
223 in order to express, by integration, *f'* as a function of *t*:

224 $$f'(T) = \frac{k(T_\infty - T_{\min})^2 t + 2j(T_\infty - T_{\min})(T_0 - T_\infty)(1 - e^{-kt}) + \frac{j^2}{2}(T_0 - T_\infty)^2(1 - e^{-2kt})}{k(T_{opt} - T_{\min})^2} \qquad (13)$$

225 The substitution of *f'* in Eq. (13) by its above-cited expression enables the calculation of the
226 equivalent temperature as follows:

227 $$T_{eq} = T_{\min} + \sqrt{\frac{k(T_\infty - T_{\min})^2 t + 2j(T_\infty - T_{\min})(T_0 - T_\infty)(1 - e^{-kt}) + \frac{j^2}{2}(T_0 - T_\infty)^2(1 - e^{-2kt})}{kt}} \qquad (14)$$

228 The implementation of the Eq. (10) to $T_{eq}$ of the thermal process yields:

229 $$\frac{N}{N_0} = \exp\left[\mu_{opt}\left(\frac{T_{eq} - T_{\min}}{T_{opt} - T_{\min}}\right)^2 t\right] \qquad (15)$$

230 The overall mathematical model corresponds to the association of these two last equations.
231 The determination of the *j* value at the centre (Eq. (4a)) or at the surface (Eq. (4b)) of an
232 infinite slab allows the calculation of the corresponding $T_{eq}$ values. The parameter *k* is

233 determined from Eq. (3) at any given position in the product and with *Bi* which includes the
234 convective heat transfer coefficient *h* that will be changed in the experimental validation of
235 the overall model.
236
237 **3. Materials and methods**
238 **3.1. Micro-organism and inoculum preparation**
239 *E. coli* SOR 201 (isolated from cheese), provided by SOREDAB Laboratory (France), was
240 stored at -80 °C in nutrient broth supplemented with 50% glycerol. The inoculum was
241 prepared by subculturing the bacterial strain in 100 mL of nutrient broth (tryptone 10 g/L,
242 meat extract 5 g/L and sodium chloride 5 g/L. pH 7.2±0.2) at 37 °C on a rotary shaker (100
243 rpm), subsequently for 8 h and 16 h.
244 **3.2. Experimental setup for the model validation at constant air temperature and**
245 **changing convective heat transfer coefficient**
246 **3.2.1. Growth measurement**
247 Growth curves were determined by the measurement of absorbance changes with a
248 spectrophotometer (Milton Roy, Spectronic 301) at 600 nm wavelength. Absorbance was
249 measured with sterile nutrient broth as a blank. Samples were filled in glass “growth flasks”
250 specially designed for the measurement of the absorbance of the content without sampling. A
251 calibration experiment was done to determine the correlation between viable counts and
252 absorbance data in nutrient broth permitting the estimation of the bacterial concentrations
253 from absorbance values. Samples were incubated at 30 °C in a shaking water bath and
254 bacteria were grown until stationary phase. The optical density was periodically measured and
255 one mL was simultaneously removed from the solution to be analyzed by the plate count
256 method. The experimental dataset was fitted with the exponential model proposed by Juarez
257 Tomas et al. (2002) to fit the calibration equation which can be written as follows:

$$LnN = a(OD)^b \quad (16)$$

Where $N$ is the bacterial concentration, $OD$ is the corresponding optical density (600 nm) measured at time $t$ and $a$ and $b$ are empirical parameters.

Fig. 1 depicts the experimental data and the calibration curve relating $OD$ to viable counts. Estimates of parameters $a$ and $b$ were respectively assessed to 22.8 [22.6 .. 22.9] and 0.090 [0.087 .. 0.093] ($R^2$ = 0.999 and $MSE$ = 0.009).

Francois et al. (2005) demonstrated that a temperature of 4 °C had no significant statistical effect on the linear calibration curve compared to optimal conditions ($T$ 30 °C, pH 7,4 and $a_w$ 0.995) in BHI medium. Consequently, we didn't perform the calibration experiment at other temperatures than 30 °C (the initial product temperature at all the experiments).

**3.2.2. Simulation design**

Five combinations of thickness of an infinite slab, convective heat transfer coefficient and chilling temperature were input (Fig. 2) for the calculation of thermal parameters $j$ and $k$. A simulated growth curve related to each combination was then calculated from Eqs. (14) and (15). An $h$ value of 8 W/(m$^2$.K) corresponds to the absence of fan (particularly in unventilated zones or in equipment inside which heat is transferred by natural convection) while an $h$ value of 60 W/(m$^2$.K) corresponds to a strong air fan (in the case of forced convection). Moreover, according to Kondjoyan (2006), average heat transfer coefficient values (W/(m$^2$.K)) calculated under different air velocity (0.2 – 5.0 m s$^{-1}$) and free-stream turbulence intensity conditions (5 – 40 %) ranged from 1.3 to 42.0 for a circular cylinder and from 2.3 to 60.0 for meat products (Beef carcass, pork hindquarter and lamb carcass (loin)). Furthermore, Ben Amara et al. (2004) studied the effect of various factors (air velocity, position, air-product temperature difference) on the transfers during cooling with a low air velocity (< 0.2 m/s), of an in-line stack of spheres and measured $h$ values ranging from 8 to 19 W/(m$^2$.K) for air velocity varying from 0.03 to 0.19 m s$^{-1}$.

### 3.2.3. Conditions of growth for the validation of the model

Corresponding to each combination of slab thickness and convective heat transfer coefficient, cooling profiles and bacterial growth were simulated at the centre and at the surface of an infinite slab shaped product. The product thermal diffusivity and thermal conductivity values input in the calculations were assumed to be equal to those of water determined at 25 °C, i.e. $1.43.10^{-7}$ $m^2/s$ and 0.6 W/(m.K) respectively.

Furthermore, input $\mu_{opt}$, $T_{min}$ and $T_{opt}$ values of *E. coli* SOR 201 were respectively equal to 2.66 $h^{-1}$, 3.28 °C and 42.03 °C in nutrient broth. These values were estimated from forty six growth kinetics conducted at 11 constant temperatures ranging from 10 °C to 46 °C. Experimental datasets were fitted and growth curve parameters (maximum growth rate ($\mu_{max}$), lag time, initial and maximum population densities) were estimated from the primary growth model of Baranyi and Roberts (1994). The obtained $\mu_{max}$ values were fitted with the secondary cardinal model (Rosso et al., 1995) in order to estimate the optimal growth rate and the cardinal temperatures of *E. coli* SOR 201 (see Fig. A2 in the appendix).

In order to validate the overall mathematical model developed in the present work, experiments were conducted under a changing temperature program which corresponds to the simulated cooling profiles of the surface or the centre of the product. All the prepared material was pre-chilled/heated to the initial temperature (30 °C). Subculture was diluted to provide an inoculation level ranging from $10^6$ to $10^7$ CFU/mL at the starting of the test. Samples were filled in glass "growth flasks" allowing the measurement of the absorbance of the content, during the experiment, without sampling. Their shaking was guaranteed by a magnetic shaking table. Samples were instantly incubated and periodically removed so as to measure optical densities (at 600 nm) in the course of the experiment. Experiments were carried out in triplicate. The chilling was monitored with a refrigerated and heating circulator (FP40-HE, Julabo Labortechnik GmbH, Germany) allowing a temperature stability of ±0.01 °C.

### 3.3. Experimental setup for the model validation at changing air temperature and constant convective heat transfer coefficient

For a further validation of the model, more complicated temperature scenarios were tested assuming alternated cooling and heating stages. Moreover, an inoculation level ranging from $10^3$ to $10^4$ CFU/mL was used in order to consider more realistic bacterial concentrations encountered in food industry processes.

Three different ambient air temperature scenarios, drawn from real refrigerated food processes, were tested (cf. Table 2).

Corresponding to each air temperature scenario, temperature profiles and bacterial growth were simulated at the centre and at the surface of an infinite slab shaped product. At all the tested temperature scenarios, the initial product temperature, the product thickness and the convective heat transfer coefficient were respectively equal to 15 °C, 0.12 m and 8 W/($m^2$.K). Input $\mu_{opt}$, $T_{min}$ and $T_{opt}$ values of *E. coli* SOR 201 are mentioned above. Typical beef meat thermal diffusivity and thermal conductivity values, respectively equal to $1.25.10^{-7}$ $m^2/s$ and 0.42 W/(m.K), were input in the calculations.

Experiments were conducted under thermal programs which corresponded to the simulated temperature profiles of the surface or the centre of the product. Subculture was diluted, samples were filled in glass “growth flasks”, instantly incubated and periodically removed so as to perform the viable count measurement in the course of the experiment. Experiments were carried out in duplicate. The thermal program was monitored with the refrigerated and heating circulator (FP40-HE, Julabo Labortechnik GmbH, Germany). At each sampling time, 1-mL aliquots were aseptically removed from each “growth flask”, serially diluted in tryptone salt broth and plated on nutrient agar (15 g/L) with a double layer. Petri dishes were incubated at 37 °C for 24 h and colonies were counted.

### 3.4. Validation and assessment of the quality of the overall model

Model accuracy was assessed by the estimation of confidence bands of predictions by using the bootstrap percentile method (Efron and Tibshirani, 1993). Forty six growth kinetics were performed in nutrient broth at 11 constant temperatures ranging from 10 °C to 46 °C (data not shown). Bootstrap of each kinetic was made in order to take the experimental errors of kinetics into account. The appropriate residuals of each kinetic were drawn with replacement. Twenty five thousands bootstrap set of primary parameters were obtained. Each set of bootstrapped $\mu_{max}$ values were used to fit the secondary model. Then bootstrapped values of parameters $T_{min}$, $T_{\text{opt}}$ and $\mu_{opt}$ were used to predict the bacterial growth with the overall model. Secondary observed residuals were drawn with replacement and added to the $\mu$ predicted value. Primary residuals were added to the predicted kinetics to consider the experimental error of cell number estimation. Twenty five thousands bootstrapped growth kinetics were obtained for each validation experiment and sorted in ascending order at each calculation time. The quartiles 2.5% and 97.5% of the sorted bootstrapped kinetics were taken to give the inferior and superior limits. These points were linked to give an approximation of the 95 percent confidence bands of the predicted growth kinetics. To validate the assumptions made and the model, less than 5% of the points must fall outside the confidence bands.

With regard to the assessment of the quality of the overall model predictions various statistical criteria were calculated at all the tested conditions of validation experiments. Correlation coefficients ($R$) between observations and predictions were calculated using the 'corrcoef' function of MATLAB 6.5. The correlation coefficient is related to the covariance *cov* by:

$$R(i,j) = \frac{\text{cov}(i,j)}{\sqrt{\text{cov}(i,i)\text{cov}(j,j)}} \qquad (17)$$

where $i$ is the observations index and $j$ is the variables index.

Bias factor $B_f$ (Eq. (18)) and Accuracy factor $A_f$ (Eq. (19)) were calculated as proposed by Jeyamkondan et al. (2001). These factors were initially introduced by Ross (1996) but here, the predicted values are normalized.

$$B_f = 10^{\sum \log(P/O)/n} \quad (18)$$

$$A_f = 10^{\sum |\log(P/O)|/n} \quad (19)$$

where $O$ and $P$ are observed and predicted microbial populations in $\log_{10}$ CFU/mL and $n$ is the number of observations. The bias factor indicates the relative average deviation of predicted and observed bacterial growth. However it has to be kept in mind that this deviation does not directly concern the size of the population, but its logarithmic transformation which reduces the effect of outliers.

A bias factor of 1 indicates perfect agreement between observed and predicted values. However, $B_f > 1$ or $< 1$ indicates that the model predicts $N$ upper than or lower than observed values. ~~For example, $B_f$ = 1.1 means that predictions are on average upper than observed values by 10%.~~ The accuracy factor gives indication of the spread of the results about the predicted value. An accuracy factor of 1 represents perfect agreement between observed and predicted values. This parameter quantifies the difference between observed and predicted values. ~~For example, $A_f$ = 1.25 indicates that the average deviation of the predicted values from the observed values is 25%. It has to be kept in mind that this deviation does not directly concern the size of the population, but its logarithmic transformation.~~

## 4. Results

### 4.1. Model validation at constant air temperature and changing convective heat transfer coefficient

#### 4.1.1. Growth simulation

Thermal programs tested at the validation stage were utilized at five different combinations of product thickness ($E$), convective heat transfer coefficient ($h$) and refrigeration temperature

($T_\infty$) (Fig. 2).

The obtained cooling profiles and growth predictions are presented in Fig. 3. As a rule, bacterial growth kinetics were faster at the product centre than at its surface. In cases of lowest thickness, simulated computing profiles (1c and 2c) were practically identical leading to the same bacterial growth predictions (1g and 2g) at the centre and at the surface of the product. In fact, in these two experiments the product thickness was sufficiently low to prevent a clear observation of an internal temperature gradient and the internal heat resistance may had been neglected. In contrast, the difference between simulated theoretical temperature kinetics at the centre and the surface of the product were more marked in the cases of the highest thickness leading to an important thermal gradient within the product (3c and 4c). For that matter, the most important differences between internal and surface growth kinetics were obtained in these two cases (3g and 4g), particularly in the case of low heat transfer coefficient.

On the other hand, additional simulated growth curves at constant temperatures equal to $T_\infty$ were presented in Fig. 3. The aim of these further experiments was to compare the bacterial growth that really occurs when temperature dynamic changes at the centre and at the surface of the cooled product are considered, with the growth that would occur if external and internal resistances were neglected.

**4.1.2. Validation results**

Each validation experiment regarding each ($T_\infty$, $h$, $E$) combination (Fig. 2) was conducted under two different refrigeration programs which corresponded to the simulated cooling of the surface and the centre of the infinite slab-shaped product yielding a total of eight validation tests. These tests lasted 24 hours with an initial temperature $T_0$ of 30 °C. In order to validate the overall mathematical model, Fig. 4 depicts predicted and observed *E. coli* SOR 201 growth during the simulated cooling at the centre or the surface of the product for the five

cases presented in Fig. 2. A fair agreement between predicted and observed growth can be noted, and the observed growth data of *E. coli* SOR 201 were found to be adequately predicted by the overall mathematical model. For each predicted growth kinetic, 95 percent confidence bands calculated with bootstrap method are also presented in Fig. 4. All the experimental data fell inside the confidence bands showing that the overall model was successfully validated at the tested conditions.

On the other hand, the quality of the overall model prediction was assessed by the calculation of correlation coefficient, $B_f$ and $A_f$ (see Table 3). The correlation coefficients were higher than 0.975 showing that the bacterial growth was satisfactorily predicted by the overall model. At all the instances, bias factors ranged from 0.98 to 1.00 indicating that ~~on average, the observed growth was at the most 2% higher than the predicted growth and that~~ the overall predictions agreed well with observed data with a slight under-prediction tendency by the model. ~~In all the tested conditions, the percentage of predicted values which were different (either above or below) than the observed values was at the most equal to 5% as can be noted from Af values ranging from 1.01 to 1.05.~~

Agreement between model predictions and experimental validation results was also assessed by plotting predicted bacterial growth versus observed bacterial growth (Fig. 5). A perfect agreement between predicted and measured growth was observed for 30.80% of experimental data. A percentage of 25.36% of the observed–predicted values' pairs were laying under the line of equivalence while 43.84% were laying above the line of equivalence.

### 4.2. Model validation at changing air temperature and constant convective heat transfer coefficient

#### 4.2.1. Growth simulation

Fig. 6 illustrates the simulated thermal profiles and bacterial growth kinetics according to the conditions presented in Table 2 and §3.3. Thermal and bacterial growth simulation results

showed important differences of temperature profiles and growth between the product centre, the product surface and the ambient air. During heating, the highest bacterial growth was observed when simulations were carried out at air temperature, followed by the product's surface and then by the product's centre. Conversely, an opposite trend was observed during cooling. From a safety point of view, neglecting heat transfer phenomena that occur inside the product and between the ambient air and the product is more dangerous at cooling stages than at heating stages. Nevertheless this hazard depends on the temperature and duration history of the cooling/heating stages. Consequently it's very important to take into account the actual temperature of the product surface or centre rather than the ambient air temperature for a reliable bacterial growth prediction.

#### 4.2.2. Validation results

Validation results regarding the three tested ambient scenarios are presented in figures 7 and 8. The observed growth data of *E. coli* SOR 201 were found to be adequately predicted by the overall mathematical model. On the other hand, less than 5% of the experimental data fell outside the 95 percent confidence bands showing that the overall model was successfully validated at the tested conditions. Table 4 presents the statistical criteria related to the data of validation at changing air temperature and shows correlation coefficients higher than 0.944 at all the tested conditions. Bias factors obtained at all the assays were higher than 1 showing a slight over-prediction tendency by the model. $A_f$ values (lower than 1.13 at all the instances) indicate that the overall predictions agreed well with observed data. Fig. 8 shows predicted bacterial growth versus observed bacterial growth and confirms that the overall model was successfully validated, with a slight over-prediction tendency, for the tested dynamic refrigeration cycles.

## 5. Discussion

Traditionally, when simulating a bacterial growth during a product cooling or heating, predictive microbiology took only the ambient air temperature into account, ignoring delays and temperature gradients due to external and internal thermal resistances linked to the effects of the medium thickness and of the convective heat transfer coefficient on the rate of heat transfer. All the studies cited in Table 1 have evaluated the prediction of bacterial growth under dynamic temperature conditions taking into account only the temperature of the cooling/heating medium. Assuming that the bacterial growth directly occurs at the temperature of air is not valid. In fact, the local temperature at any given position in the product depends upon both $T_\infty$ and $h$. In the present study, predictive microbiology was combined with heat transfer phenomena in order to develop an overall mathematical model describing the effect of the ambient temperature and the convective heat transfer coefficient on bacterial growth. The proposed method in this work is different than those in previous studies which combined predictive microbiology and heat transfer (Alavi et al., 2001; Amezquita et al., 2005; Bellara et al., 2000; Corradini et al., 2006). An experimental method was implemented in order to validate the model results. Thermal profiles were firstly simulated at the centre and at the surface of the infinite slab shaped product. Then, experiments were conducted under a changing temperature program corresponding to the simulated temperature kinetics. The validation of the overall model was performed by the comparison of the measured bacterial growths with model predictions at constant ambient air temperature and changing convective heat transfer coefficient and product thickness (five different combinations of product thickness, convective heat transfer coefficient and cooling air temperature were tested), then at changing ambient air temperature and fixed convective heat transfer coefficient and product thickness (three different ambient air scenarios assuming alternated cooling and heating stages, drawn from real refrigerated food processes, were tested).

As expected, the results of the computer simulation related to single cooling stage experiments showed that the bacterial growth kinetics were faster at the product centre than at its surface. Moreover, the importance of the impact of the convective heat transfer coefficient and of the product thickness on the bacterial growth during the cooling of an infinite slab shaped product by pulsed air was pointed out. As an example, at the product half thickness, the level of bacterial growth accomplished after 5 hours of cooling with $h$ = 8 W/(m$^2$.K) (case 3) was the same after 16.5 hours with $h$ = 60 W/(m$^2$.K) (case 4). For these cases the product thickness was the same and the cooling air temperature was in case 3 4°C lower than in case 4. Similarly, at product half thickness, the cooling time needed to reach a same bacterial growth with low or high product thickness (1 cm in case 2 and 6 cm in case 4) was estimated to 17.5 hours and 8 hours, respectively, for the same convection level (60 W/(m$^2$.K)). The slowest simulated bacterial growth was observed with intermediate product thickness and convective heat transfer coefficient (case 5). Moreover, it obviously appears that the validity of the assumption of an instantaneously thermal equilibrium between the product and the cooling medium with regard to bacterial growth is depending on the level of convection. In fact, predicted growth kinetics at the surface of the product were close to those predicted at $T_\infty$ for high heat transfer coefficients ($h$) equal to 60 W/(m$^2$.K), which corresponds to a strong air fan (Fig. 3: 2g and 4g). At this instance, neglecting the external heat resistance may be accepted particularly for low product thickness (1 cm) where there's no internal heat resistance too. Oppositely, for low heat transfer coefficients ($h$) equal to 8 W/(m$^2$.K), which corresponds to the absence of fan, (Fig. 3: 1g and 3g) important dissimilarities between predicted growth kinetics at the surface of the product and at $T_\infty$ may be observed. Indeed, assuming no external heat transfer resistance is not valid especially for high product thickness of 6 cm (Fig. 3: 3g) where the bacterial growth that occurs when the product is cooled from $T_0$ to $T_\infty$ was clearly higher than that at an immediately reached temperature $T_\infty$. In this case, a

505 difference of 1.35 $\log_{10}$(CFU/mL) between the bacterial populations at the product surface
506 and at $T_\infty$ was reached after 24 hours of growth. Besides, using the bootstrap percentile
507 method for the estimation of confidence bands of predictions, the model was successfully
508 validated at all the tested conditions.
509 Concerning the results related to alternated cooling and heating stage experiments, the model
510 was successfully validated at more complicated ambient air scenarios and lower inoculation
511 levels by plate count measurement method. These results showed that, in predictive
512 microbiology, assuming an instantaneously thermal equilibrium between the product and the
513 ambient medium is not valid and may have large consequences on risk assessment of
514 refrigerated food processes (see Fig. 9).
515 To assess the quality of the overall model, predicted bacterial growth was compared to
516 observed growth according to several statistical criteria related to the data of validation. Our
517 results pointed out a good agreement between predicted and observed growth.
518 On the other hand, in the overall model, as a primary bacterial model, a simple exponential
519 growth without lag time was assumed. In other words, it is supposed that the bacterial growth
520 occurred without delay when the product temperature was continuously changing. Our
521 assumption is in agreement with several previous studies. Although the fact that organisms
522 need to adapt to the new temperature, so that they go through a lag phase caused by the stress
523 of the temperature shift, was largely noticed in literature (Amezquita et al., 2005; Baranyi et
524 al., 1995; Koutsoumanis, 2001; Zwietering et al., 1994), the lag phase duration was rarely
525 considered in predictive models. In accordance with our work, no further delay occurring after
526 temperature shifts, once a cell population is growing exponentially, was frequently assumed
527 (Baranyi et al., 1995; Bovill et al., 2000; Koutsoumanis et al., 2006). Although, Swinnen et al.
528 (2005) demonstrated that temperature shifts crossing a lag/no lag transition zone (positioned
529 more or less between 22.78 and 23.86 °C for *E. coli* K12 MG1655) will cause an intermediate

lag phase, we consider that neglecting contingent intermediate lag phase by our model may be a valid approach. In fact, simulated thermal profiles at product surface or centre due to heat transfer phenomena (see Fig. 3 and Fig. 6) progressively changed with time and cannot be regarded as instantaneous temperature shifts with given amplitude which may generate intermediate lag phases.

Paradoxically, the complexity of foods' shapes and the lack of knowledge about their physical properties dictate the utilization of simple model. We took as an example the case of infinite slab, but the model can be generalised to complex shapes. A classical and relevant approach is of course, the implementation of numerical modelling. Another approach is related to the well-known Ball method (Ball, 1923) with its two empirical parameters, for heat treatment processes calculations. Because foodstuffs shapes are complex and because their thermal properties are often unknown, it can be relevant to implement a simple model including only two parameters ($j$ and $k$ of Eq. (1)) which can be easily empirically estimated from a simple temperature registration and a simple linear regression of the reduced temperature (which is linearised from a logarithmic transformation). Note that errors which can be generated by "simplistic" heat transfer models are minor compared to errors which are linked to the "biological background". Moreover, the overall model can be used for any bacterial strain having known growth parameters $T_{min}$, $T_{opt}$ and $\mu_{opt}$. Accordingly, the proposed model can be used for designing safe cooling or heating processes and may be considered as a very useful tool for risk assessment regarding food safety and process optimisation.

## 6. Appendix

Equation of the the infinite series given by Carslaw and Jaeger (1986):

$$\frac{T_\infty - T}{T_\infty - T_0} = \sum_1^\infty \frac{2\sin\varphi_n}{\varphi_n + \sin\varphi_n \cos\varphi_n} \cos\left(\varphi_n \frac{x}{x_{\max}}\right) \exp\left(-\varphi_n{}^2 Fo\right) \qquad (20)$$

with $x_{max}$ is half-thickness for an infinite slab and $\varphi_n$ are the roots of the equation $\cot\varphi = \frac{\varphi}{Bi}$.

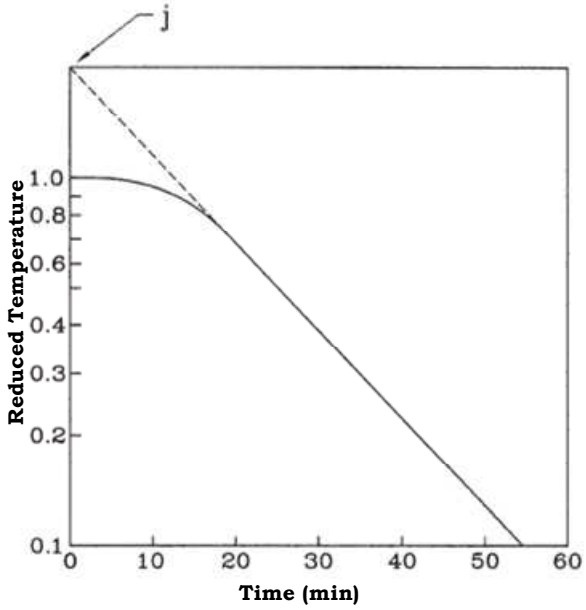


Fig. A1. Typical cooling curve (Becker and Fricke, 2004)

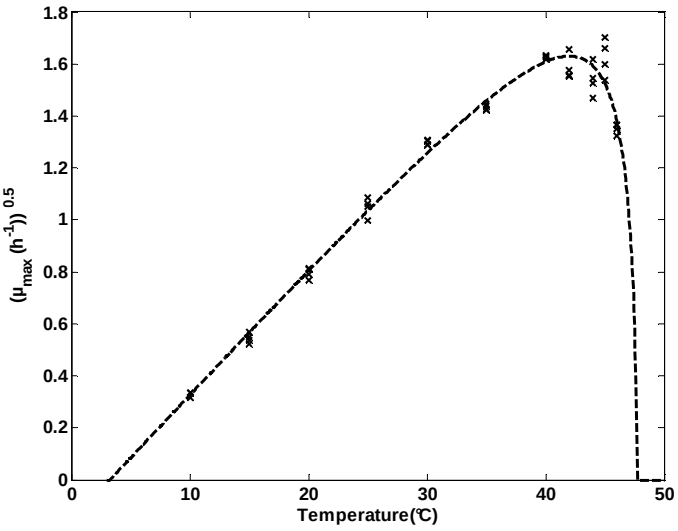


Fig. A2. Fit of the cardinal model on $\mu_{\max}$ values measured in nutrient broth (×). The dashed line denotes the fitted model on the experimental data.

560 **References**

561

562 Alavi, S.H., Puri, V.M., Mohtar, R.H. 2001. A model for predicting the growth of
563 *Listeria monocytogenes* in packaged whole milk. Journal of Food Process Engineering 24,
564 231–251.

565 Amezquita, A., Weller, C.L., Wang, L., Thippareddi, H., Burson, D.E. 2005.
566 Development of an integrated model for heat transfer and dynamic growth of *Clostridium*
567 *perfringens* during the cooling of cooked boneless ham. International Journal of Food
568 Microbiology 101, 123-144.

569 Armitage, N.H. 1997. Use of predictive microbiology in meat hygiene regulatory
570 activity. International Journal of Food Microbiology 36, 103-109.

571 Ball, C. 1923. Thermal process times for canned foods. Bulletin 7-1, 37 (National
572 Research Council, Washington, DC).

573 Baranyi, J., Roberts, T.A. 1994. A dynamic approach to predicting bacterial growth in
574 food. International Journal of Food Microbiology 23, 277-294.

575 Baranyi, J., Robinson, T.P., Kaloti, A., Mackey, B.M. 1995. Predicting growth of
576 *Brochothrix thermosphacta* at changing temperature. International Journal of Food
577 Microbiology 27, 61-75.

578 Becker, B.R., Fricke, B.A. 2004. Heat transfer coefficients for forced-air cooling and
579 freezing of selected foods. International Journal of Refrigeration 27, 540-551.

580 Bellara, S.R., McFarlane, C.M., Thomas, C.R., Fryer, P.J. 2000. The growth of
581 *Escherichia coli* in a food simulant during conduction cooling: combining engineering and
582 microbiological modelling. Chemical Engineering Science 55, 6085-6095.

583 Ben Amara, S., Laguerre, O., Flick, D. 2004. Experimental study of convective heat
584 transfer during cooling with low air velocity in a stack of objects. International Journal of
585 Thermal Sciences 43, 1213-1221.
586 Bimbenet, J.J., Duquenoy, A., Trystram, G. 2002. Génie des procédés alimentaires. Des
587 bases aux applications. Dunod ed., Paris, France.
588 Bovill, R., Bew, J., Cook, N., D'Agostino, M., Wilkinson, N., Baranyi, J. 2000.
589 Predictions of growth for *Listeria monocytogenes* and *Salmonella* during fluctuating
590 temperature. International Journal of Food Microbiology 59, 157–165.
591 Bovill, R.A., Bew, J., Baranyi, J. 2001. Measurements and predictions of growth for
592 *Listeria monocytogenes* and *Salmonella* during fluctuating temperature II. Rapidly changing
593 temperatures. International Journal of Food Microbiology 67, 131–137.
594 Caro-Corrales, J., Cronin, K., Abodayeh, K., Gutiérrez-López, G., Ordorica-Falomir, C.
595 2002. Analysis of random variability in biscuit cooling. Journal of Food Engineering 54, 147-
596 156.
597 Carslaw, H.S., Jaeger, J.C. 1986. Conduction of Heat in Solids. 2nd ed. Oxford
598 University Press.
599 Corradini, M.G., Amézquita, A., Normand, M.D., Peleg, M. 2006. Modeling and
600 predicting non-isothermal microbial growth using general purpose software. International
601 Journal of Food Microbiology 106, 223–228.
602 Dalgaard, P. 1995. Modelling of microbial activity and prediction of shelf life for
603 packed fresh fish. International Journal of Food Microbiology 26, 305-317.
604 de Jong, A.E.I., Beumer, R.R., Zwietering, M.H. 2005. Modeling growth of *Clostridium*
605 *perfringens* in pea soup during cooling. Risk Analysis: An International Journal 25, 61-73.
606 Dincer, I. 1996. An exact solution on the estimation of heat-transfer rates during deep-
607 freezing of slab products. Journal of Food Engineering 30, 417-423.

608 Efron, B., Tibshirani, R.J. 1993. Confidence intervals based on bootstrap percentiles. In:
609 An introduction to the Bootstrap. Chapman and Hall, New York, pp. 168-177.
610 Erdogdu, F. 2005. Mathematical approaches for use of analytical solutions in
611 experimental determination of heat and mass transfer parameters. Journal of Food
612 Engineering 68, 233-238.
613 Francois, K., Devlieghere, F., Standaert, A.R., Geeraerd, A.H., Cools, I., Van Impe,
614 J.F., Debevere, J. 2005. Environmental factors influencing the relationship between optical
615 density and cell count for *Listeria monocytogenes*. Journal of Applied Microbiology 99, 1503-
616 1515.
617 Fujikawa, H., Kai, A., Morozumi, S. 2004. A new logistic model for *Escherichia coli*
618 growth at constant and dynamic temperatures. Food Microbiology 21, 501–509.
619 Gibson, A.M., Bratchell, N., Roberts, T.A. 1987. The effect of sodium chloride and
620 temperature on the rate and extent of growth of *Clostridium botulinum* type A in pasteurized
621 pork slurry. Journal of Applied Bacteriology 62, 479-490.
622 Gill, C.O., Harrison, J.C.L. 1985. Evaluation of the hygienic efficiency of offal cooling
623 procedures. Food Microbiology 2, 63-69.
624 Gumudavelli, V., Subbiah, J., Thippareddi, H., Velugoti, P.R., Froning, G. 2007.
625 Dynamic predictive model for growth of *Salmonella Enteritidis* in egg yolk. Journal of Food
626 Science 72, M254-M262.
627 Huang, L. 2003. Dynamic computer simulation of *Clostridium perfringens* growth in
628 cooked ground beef. International Journal of Food Microbiology 87, 217–227.
629 Jeyamkondan, S., Jayas, D.S., Holley, R.A. 2001. Microbial growth modelling with
630 artificial neural networks. International Journal of Food Microbiology 64, 343-354.
631 Juarez Tomas, M.S., Bru, E., Wiese, B., de Ruiz Holgado, A.A.P., Nader-Macias, M.E.
632 2002. Influence of pH, temperature and culture media on the growth and bacteriocin

633 production by vaginal *Lactobacillus salivarius* CRL 1328. Journal of Applied Microbiology
634 93, 714-724.
635 Juneja, V.K., Marks, H., Thippareddi, H. 2008. Predictive model for growth of
636 *Clostridium perfringens* during cooling of cooked uncured beef. Food Microbiology 25, 42-
637 55.
638 Kondjoyan, A. 2006. A review on surface heat and mass transfer coefficients during air
639 chilling and storage of food products. International Journal of Refrigeration 29, 863-875.
640 Koseki, S., Isobe, S. 2005. Prediction of pathogen growth on iceberg lettuce under real
641 temperature history during distribution from farm to table. International Journal of Food
642 Microbiology 104, 239–248.
643 Koutsoumanis, K. 2001. Predictive modeling of the shelf life of fish under
644 nonisothermal conditions. Applied and Environmental Microbiology 67, 1821–1829.
645 Koutsoumanis, K., Stamatiou, A., Skandamis, P., Nychas, G.J.E. 2006. Development of
646 a microbial model for the combined effect of temperature and pH on spoilage of ground meat,
647 and validation of the model under dynamic temperature conditions. Applied and
648 Environmental Microbiology 72, 124-134.
649 Lebert, I., Lebert, A. 2006. Quantitative prediction of microbial behaviour during food
650 processing using an integrated modelling approach: a review. International Journal of
651 Refrigeration 29, 968-984.
652 Mafart, P. 1997. Génie industriel Alimentaire. Tome 1: Les procédés physiques de
653 conservation. Lavoisier Techniques & Documentations ed., Paris, France.
654 Mafart, P. 2005. Food engineering and predictive microbiology: on the necessity to
655 combine biological and physical kinetics. International Journal of Food Microbiology 100,
656 239-251.

McMeekin, T.A., Brown, J., Krist, K., Miles, D., Neumeyer, K., Nichols, D.S., Olley, J., Presser, K., Ratkowsky, D.A., Ross, T., Salter, M., Soontranon, S. 1997. Quantitative Microbiology: A Basis for Food Safety. Emerging Infectious Diseases 3, 541-550.

McMeekin, T.A., Olley, J.N., Ross, T., Ratkowsky, D.A. 1993. Predictive Microbiology: theory and application Research Studies Press, Taunton, Somerset, England.

Ratkowsky, D.A., Olley, J., McMeekin, T.A., Ball, A. 1982. Relationship between temperature and growth rate of bacterial cultures. Journal of Bacteriology 149, 1-5.

Ross, T. 1996. Indices for performance evaluation of predictive models in food microbiology. Journal of Applied Bacteriology 81, 501-508.

Rosso, L., Lobry, J.R., Bajard, S., Flandrois, J.P. 1995. Convenient model to describe the combined effects of temperature and pH on microbial growth. Applied and Environmental Microbiology Vol. 61, p. 610–616.

Swinnen, I.A.M., Bernaerts, K., Gysemans, K., Van Impe, J.F. 2005. Quantifying microbial lag phenomena due to a sudden rise in temperature: a systematic macroscopic study. International Journal of Food Microbiology 100, 85.

U.S.D.A. 1999. Performance standards for the production of certain meat and poultry products. Final rule. Federal Register 64, 732-749.

Zwietering, M.H., De Koos, J.T., Hasenack, B.E., De Wit, J.C., Van't Riet, K. 1991. Modeling of bacterial growth as a function of temperature. Applied and Environmental Microbiology 57, 1094-1101.

Zwietering, M.H., De Wit, J.C., Cuppers, H.G.A.M., Van't Riet, K. 1994. Modeling of bacterial growth with shifts in temperature. Applied and Environmental Microbiology 60, 204-213.

Zwietering, M.H., Hasting, A.P.M. 1997. Modelling the hygienic processing of foods - Influence of individual process stages. Food and Bioproducts Processing 75, 168-173.

682 Zwietering, M.H., Wijitzes, T., de Wit, J.C., Van't Riet, K. 1992. A decision support
683 system for prediction of the microbial spoilage in foods. Journal of Food Protection 55, 973-
684 979.
685
686

**Figure captions**

Fig. 1.

Calibration curve between viable counts and absorbance data depicted with solid line. Experimental data measured at 30°C in nutrient broth are marked with (o).

Fig. 2.

Experimental design implemented for the validation of the overall model at different combinations (mentioned with numbers from 1 to 5) of product thickness ($E$), convective heat transfer coefficient ($h$) and refrigeration temperature ($T_\infty$).

Fig. 3.

Cooling scenarios (from 1c to 5c) and bacterial growth curves (from 1g to 5g) obtained from simulation of the overall model at the five cases of the experimental design. Symbols in predicted cooling profiles: temperature of product centre (line —) and temperature of product surface (line — · —). Symbols in predicted growth curves: bacterial growth at product centre (line —), bacterial growth at product surface (line — · —) and bacterial growth that occurs at $T_\infty$ (line **.....**).

Fig. 4.

Comparison of predicted and observed *Escherichia coli* SOR 201 growth during cooling. ***a***: case1 at the centre or the surface of the product. ***b***: case2 at the centre or the surface of the product. ***c***: case3 at the product centre. ***d***: case3 at the product surface. ***e***: case4 at the product centre. ***f***: case4 at the product surface. ***g***: case5 at the product centre. ***h***: case5 at the product surface. Symbols in experimental data: o, □, Δ. Predicted growth curves estimated by the overall model are presented with (line —). 95 percent confidence bands obtained with bootstrap method are presented with (line — —).

720 Fig. 5.

721

722 Predicted bacterial growth from the overall model versus observed bacterial growth obtained
723 with constant air temperature. Symbols: □ (case 1), o (case 2). Symbols related to product
724 surface experiments: ∗ (case 3), Δ (case 4), ◊ (case 5). Symbols related to product centre
725 experiments: • (case 3), + (case 4), x (case 5). The line of equivalence between predicted and
726 observed growth is marked with (line —).

727

728 Fig. 6.

729

730 Thermal profiles (from 1c to 3c) and bacterial growth curves (from 1g to 3g) obtained by
731 simulation of the overall model at the three ambient air scenarios. Symbols in predicted
732 cooling profiles: temperature of product centre (line —) and temperature of product surface
733 (line — · —). Symbols in predicted growth curves: bacterial growth at product centre (line
734 —), bacterial growth at product surface (line — · —) and bacterial growth that occurs at $T_\infty$
735 (line **.....**).

736

737 Fig. 7.

738

739 Comparison of predicted and observed *Escherichia coli* SOR 201 growth during thermal
740 processing at changing air temperature. ***a***, ***c*** and ***e*** depict the model validation results at the
741 product centre according to cycle N°1, cycle N°2 and cycle N°3, respectively. ***b***, ***d*** and ***f***
742 depict the model validation results at the product surface according to cycle N°1, cycle N°2
743 and cycle N°3, respectively. Symbols in experimental data: o, □. Predicted growth curves
744 estimated by the overall model are presented with (line —). 95 percent confidence bands
745 obtained with bootstrap method are presented with (line — —).

746

747 Fig. 8.

748 Predicted bacterial growth from the overall model versus observed bacterial growth obtained
749 with changing air temperature. Symbols related to product surface experiments: □ (Cycle
750 N°1), ∗ (Cycle N°2), Δ (Cycle N°3). Symbols related to product centre experiments: o (Cycle
751 N°1), • (Cycle N°2), + (Cycle N°3). The line of equivalence between predicted and observed
752 growth is marked with (line —).

753 Fig. 9.

754 Comparison of the bacterial growth prediction at ambient temperature according to cycle N°1
755 with the model validation results at product's centre (***a***) and at product's surface (***b***). Symbols
756 in experimental data: o, □. Symbols in predicted growth curves: bacterial growth at product's
757 surface or centre (line —), bacterial growth that occurs at $T_\infty$ (line **.....**). 95 percent confidence
758 band of predictions at $T_\infty$ obtained with bootstrap method is presented with (line — —).

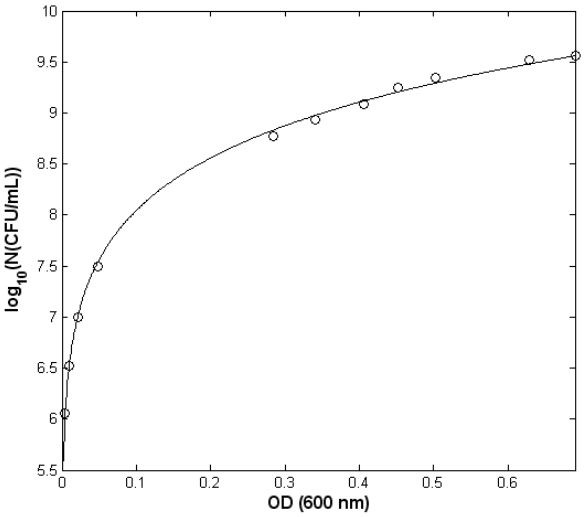


Fig. 1.

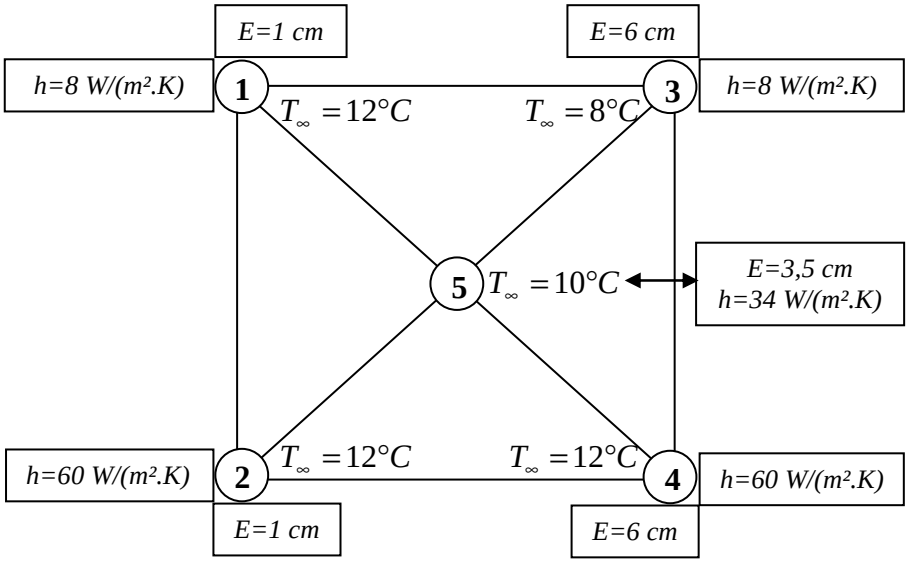
E=1 cm
E=6 cm
h=8 W/(m².K)
1
$T_\infty = 12°C$
$T_\infty = 8°C$
3
h=8 W/(m².K)
5
$T_\infty = 10°C$
E=3,5 cm
h=34 W/(m².K)
h=60 W/(m².K)
2
$T_\infty = 12°C$
$T_\infty = 12°C$
4
h=60 W/(m².K)
E=1 cm
E=6 cm

Fig. 2.

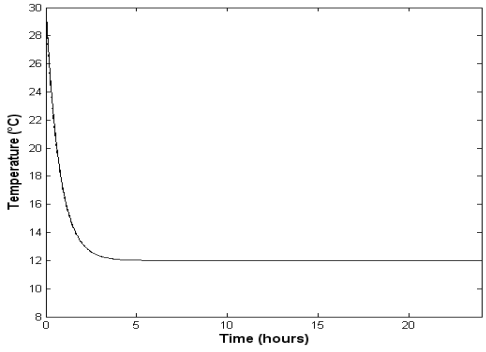


*1c*

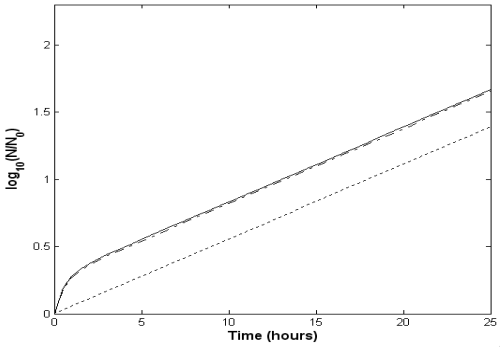


*1g*

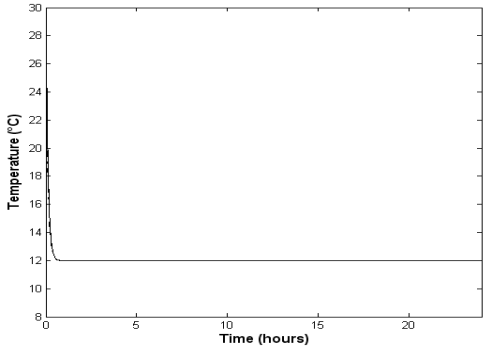


*2c*

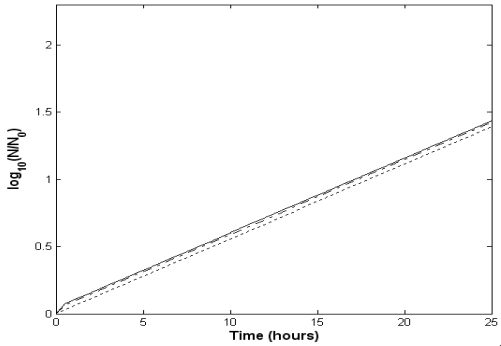


*2g*

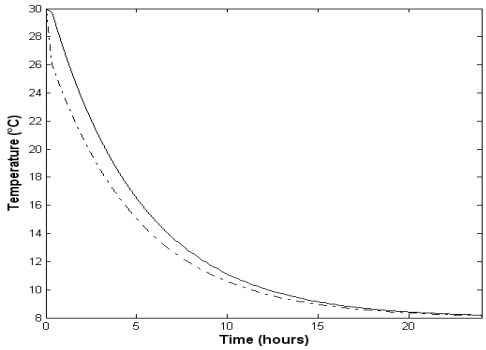


*3c*

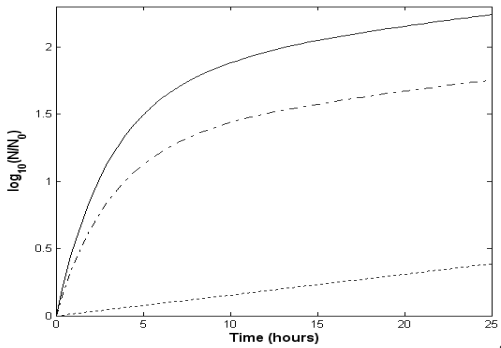


*3g*

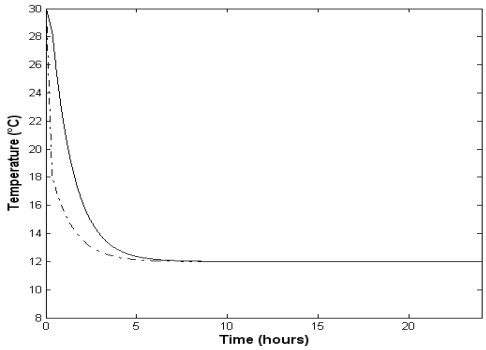


*4c*

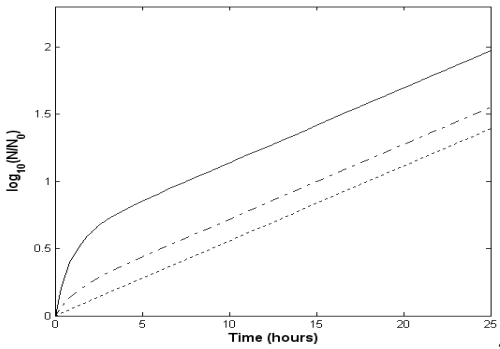


*4g*

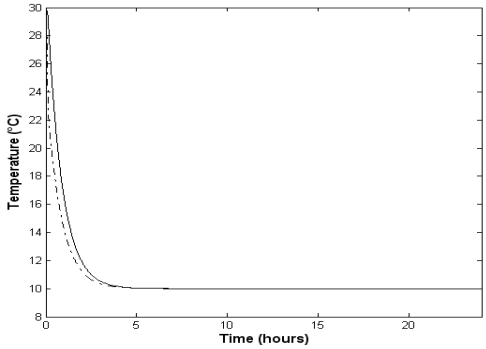


*5c*

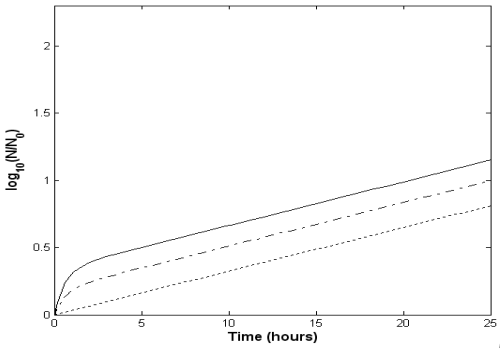


*5g*

783 Fig. 3.

784

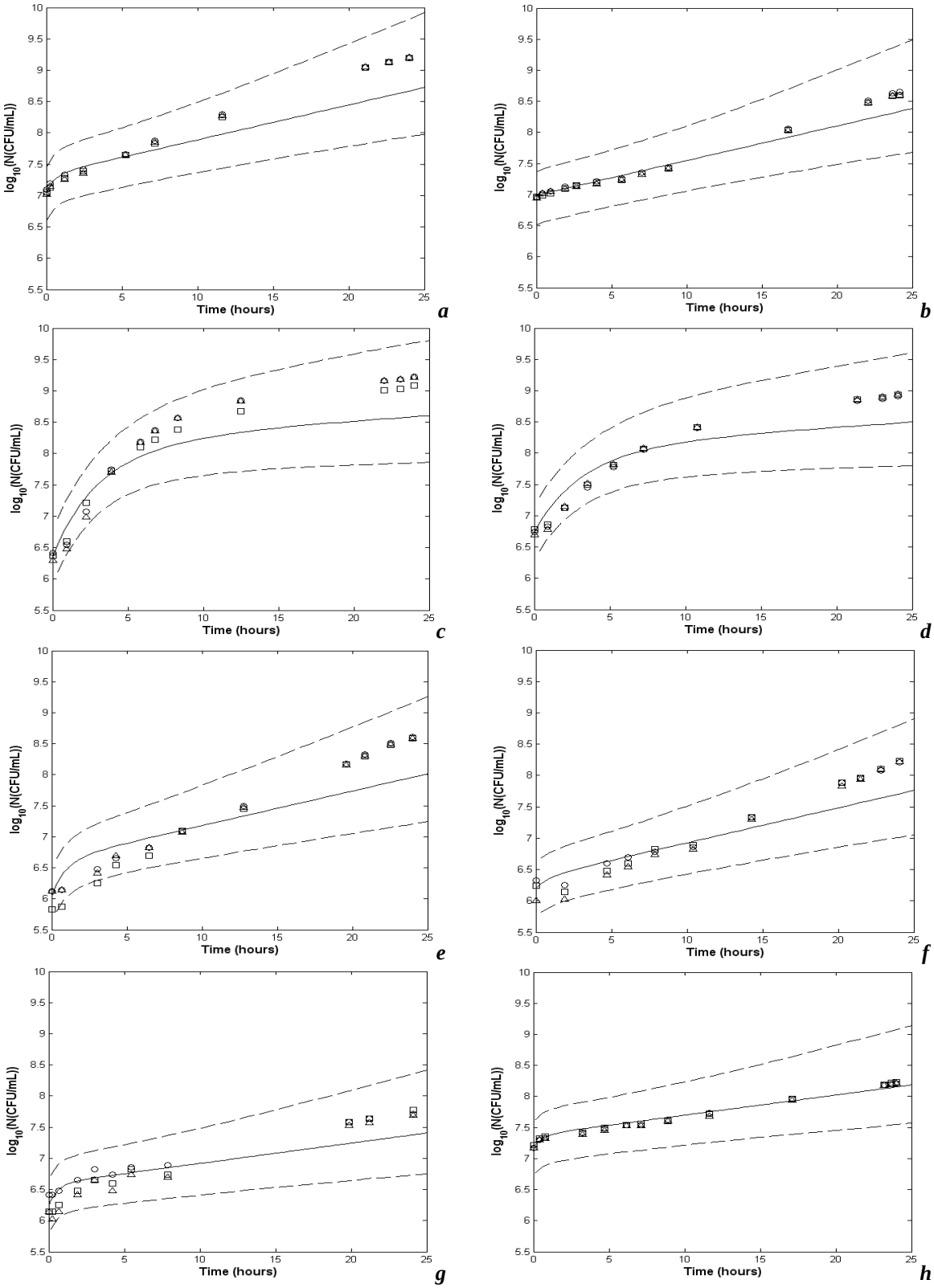


785 Fig. 4.

786

787

788

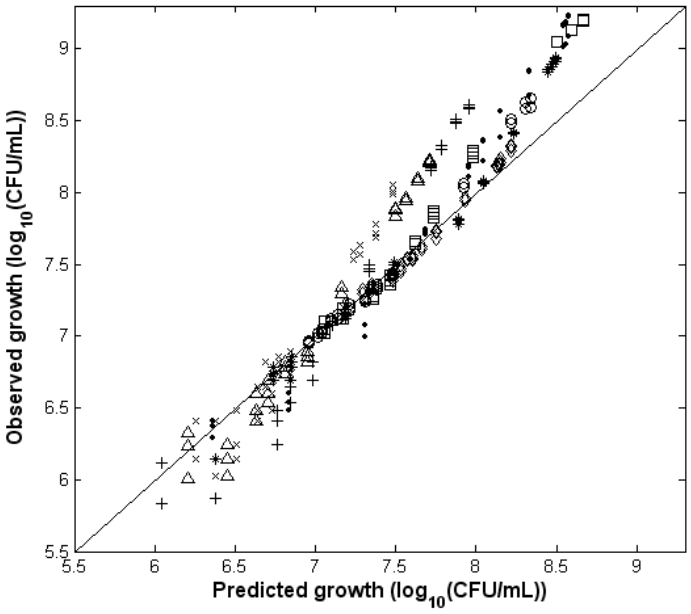


789

790 Fig. 5.

791

792

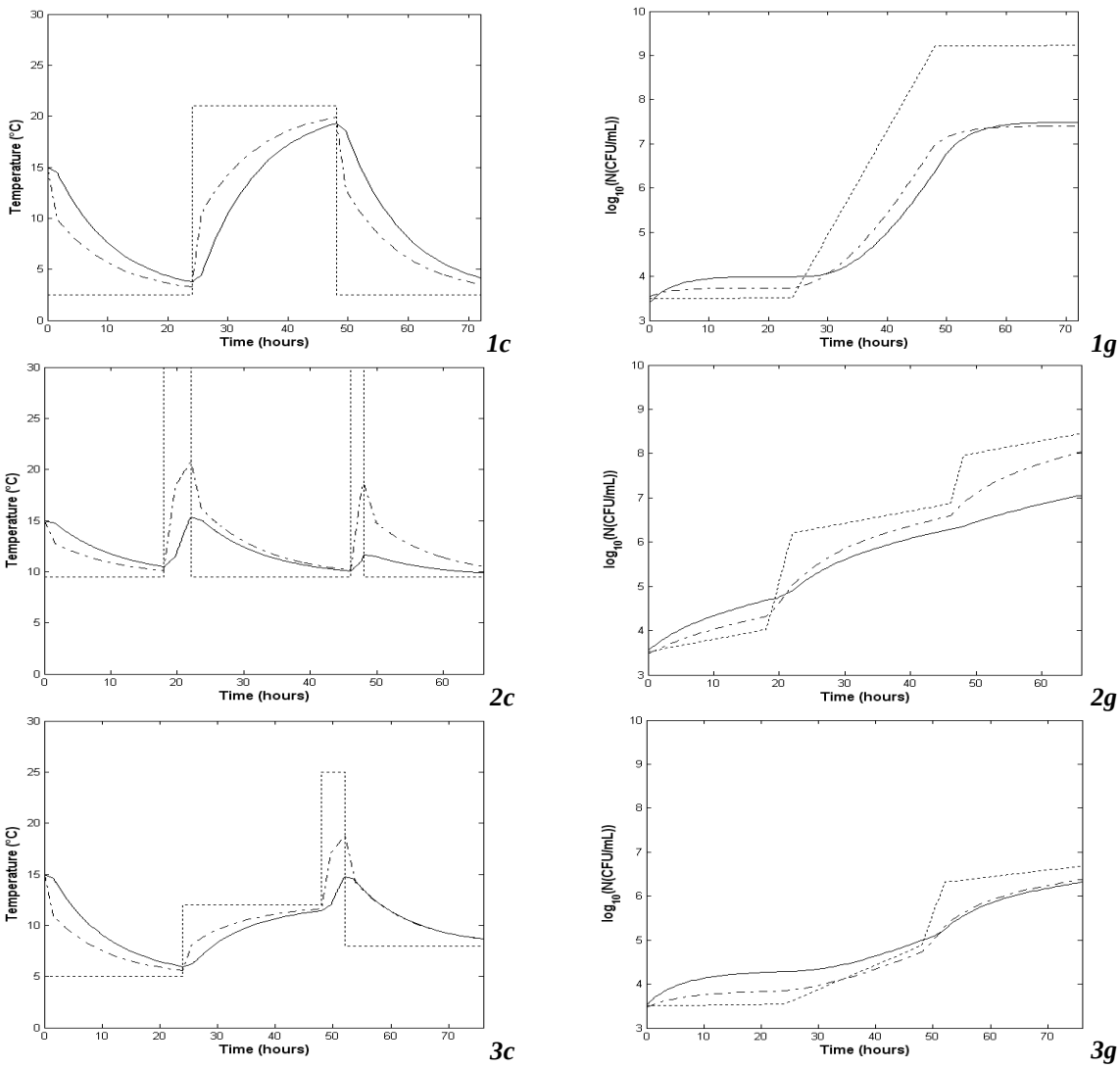
Temperature (°C)
Time (hours)
log10(N(CFU/mL))
Time (hours)
1c
1g
2c
2g
3c
3g

793 Fig. 6.

794

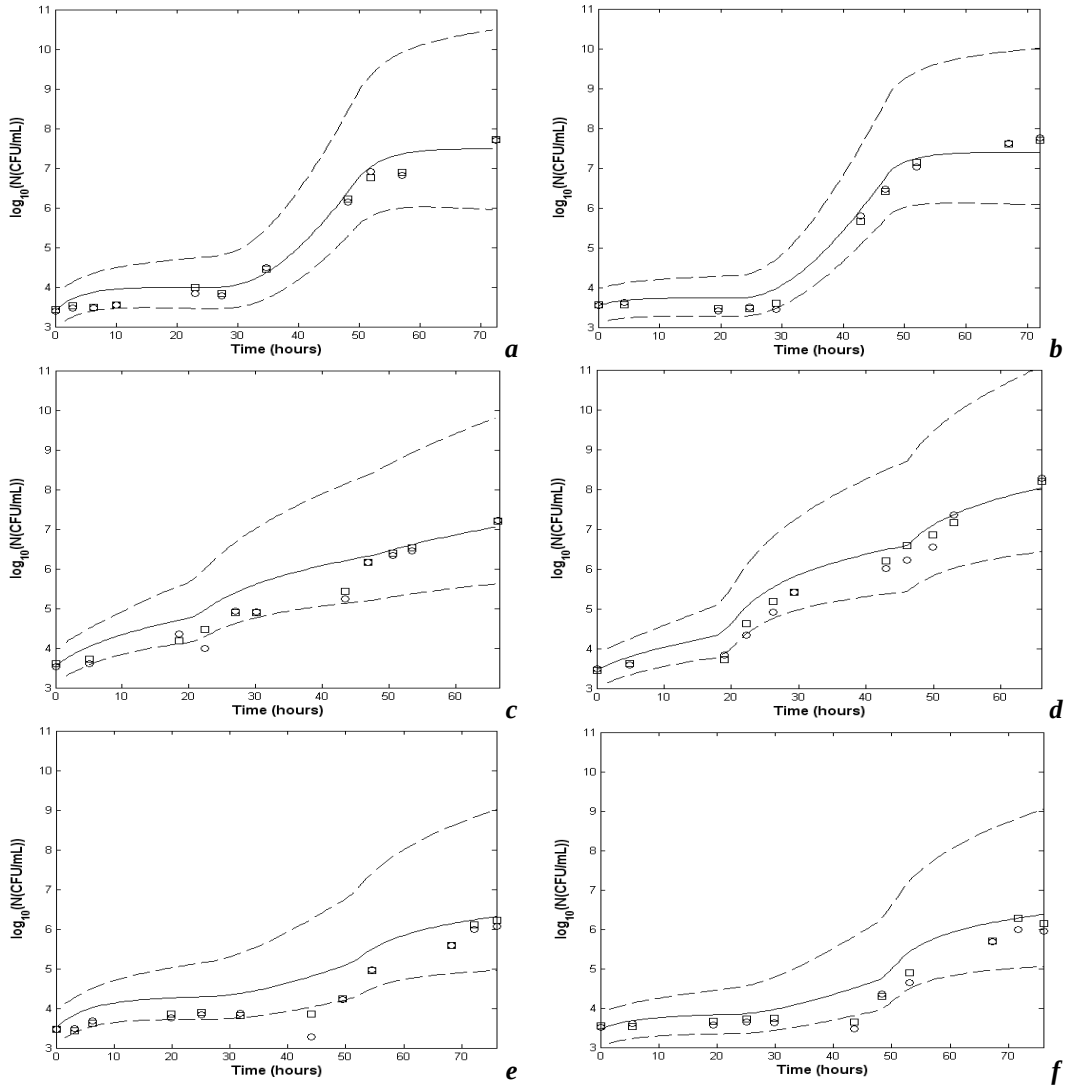


795 Fig. 7.

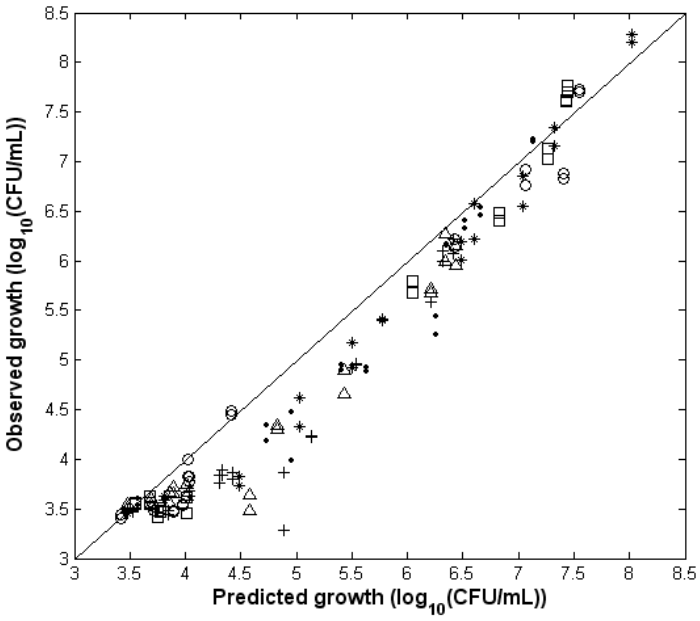
Observed growth (log10(CFU/mL))
Predicted growth (log10(CFU/mL))
8.5
8
7.5
7
6.5
6
5.5
5
4.5
4
3.5
3
3
3.5
4
4.5
5
5.5
6
6.5
7
7.5
8
8.5

796

797 Fig. 8.

798

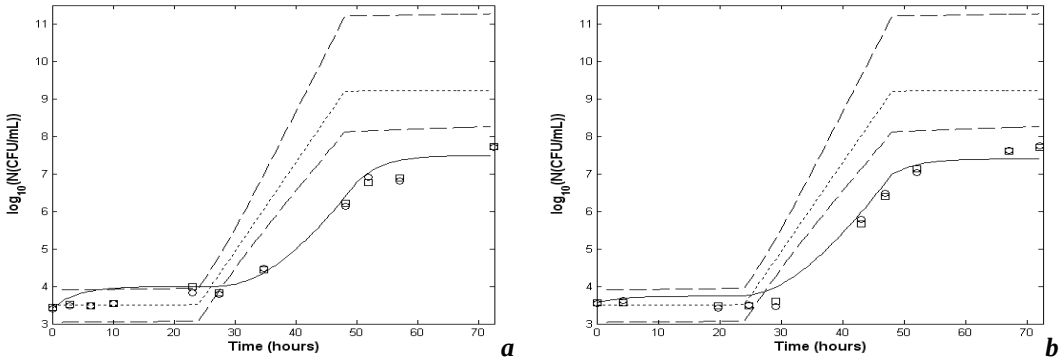


799

800

801 Fig. 9.

802

803 Table 1

804 List of previous works dealing with models predicting the bacterial growth under dynamic

805 temperature conditions

806

| y Model | Secondary model | Solution method | Validation conditions | R |
|---|---|---|---|---|
| nd Roberts aranyi and 4). | Quadratic polynomial model. | Numerical solution by the fourth order Runge–Kutta method. | Rates of change of T ranging from 1.7°C.h$^{-1}$ to a virtually instantaneous change: cooling from 25°C to -2, 2, 5 or 10°C and heating from 2°C to 25°C. | Bovil |
| gistic model. | Arrhenius equation. | Numerical solution by the fourth order Runge–Kutta method. | Various types of a dynamic temperature history with various intervals were studied for of *Escherichia coli* 1952 growth prediction. | Fujik 2004 |
| nd Roberts aranyi and 4). | A modified Ratkowsky equation (Zwietering et al., 1991). | Numerical solution by the fourth order Runge–Kutta method. | Growth of *Salmonella Enteritidis* in egg yolk under varying temperature profiles (exponential and linear cooling, exponential heating and sinusoidal temperatures). | Gumu al., 2 |
| form of the odel (Gibson | A modified Ratkowsky equation (Zwietering et al., 1991). | Numerical solution by the fourth order Runge–Kutta method. | Growth of *Clostridium perfringens* in cooked ground beef under fluctuating temperature conditions between 30°C and 45°C (square waved) and under continuous temperature changes from 51°C to 10°C (linear and exponential cooling). | Huan |

807 Table 2

808 Tested temperature scenarios for the validation of the model at changing air temperature and

809 constant convective heat transfer coefficient equals to 8 W/($m^2$.K)

810

| Stage of the cycle | Temperature (°C) | Duration (h) |
|---|---|---|
| Cycle N° 1 | | |
| Storage in a cold room | 2.5 | 24 |
| Refrigeration stopped due to an accidental failure of the installation | 21 | 24 |
| Repaired breakdown and remaining product in the cold room | 2.5 | 24 |
| Cycle N° 2 | | |
| Industrial storage and transport | 9.5 | 18 |
| Household doorstep delivery | 30 | 4 |
| Storage in refrigerator | 9.5 | 24 |
| Product on the table | 30 | 2 |
| Remaining product in the refrigerator | 9.5 | 18 |
| Cycle N° 3 | | |
| Storage and transport | 5 | 24 |
| Storage in the refrigerated cabinet | 12 | 24 |
| Household doorstep delivery | 25 | 4 |
| Storage in refrigerator | 8 | 24 |

811 Table 3

812 Statistical criteria related to the data of validation at constant air temperature and changing
813 convective heat transfer coefficient

814

| Test conditions | $R$ | $B_f$ | $A_f$ |
|---|---|---|---|
| Case 1 | 0.996 | 0.98 | 1.03 |
| Case 2 | 0.996 | 0.99 | 1.01 |
| Case 3 at product centre | 0.987 | 0.98 | 1.04 |
| Case 3 at product surface | 0.987 | 0.99 | 1.02 |
| Case 4 at product centre | 0.976 | 0.99 | 1.05 |
| Case 4 at product surface | 0.986 | 0.99 | 1.03 |
| Case 5 at product centre | 0.975 | 0.99 | 1.03 |
| Case 5 at product surface | 0.994 | 1 | 1.01 |

815

816

817 Table 4

818 Statistical criteria related to the data of validation at changing air temperature and constant

819 convective heat transfer coefficient equals to 8 W/($m^2$.K)

820

| Test conditions | $R$ | $B_f$ | $A_f$ |
|---|---|---|---|
| Cycle 1 at product centre | 0.991 | 1.05 | 1.05 |
| Cycle 1 at product surface | 0.992 | 1.04 | 1.05 |
| Cycle 2 at product centre | 0.963 | 1.08 | 1.08 |
| Cycle 2 at product surface | 0.986 | 1.06 | 1.06 |
| Cycle 3 at product centre | 0.944 | 1.13 | 1.13 |
| Cycle 3 at product surface | 0.964 | 1.09 | 1.09 |

821

822

823